

## Facial Expression Recognition Using Gabor Wavelet & Neural Networks

Amira Elsir Tayfour  
King Khalid University  
Abha, Saudi Arabia  
[amtyfoor@gmail.com](mailto:amtyfoor@gmail.com)

Dr. Altahir Mohammed  
Sudan University of Science & Technologies  
Khartoum, Sudan  
[altahir\\_33@yahoo.com](mailto:altahir_33@yahoo.com)

Dr. Moawia Yahia  
King Faisal University  
Saudi Arabia  
[meyahia@hotmail.com](mailto:meyahia@hotmail.com)

**Abstract—** This paper presents methods for identifying facial expression. The objective of this paper is to present a combination texture oriented method with dimensional reduction for identifying facial expressions. Conventional methods have difficulty in identifying expressions due to change in the shape of the cheek. By using simple two dimensional image analysis, the accuracy of the expression detection becomes difficult. Without considering the three dimensional analysis, by using texture extraction of the cheek, we are able to increase the accuracy of the expression detection. In order to achieve the expression detection accuracy, Gabor wavelet is used in different angles to extract possible texture of the facial expression. The texture dimension is further reduces by using Fisher's linear discriminant function for increasing the accuracy of the proposed method. Fisher's linear discriminant function from transforming higher dimensional feature vector into two-dimensional vector training and identifying expressions. Different facial expressions considered are angry, disgust, happy, sad, surprise and fear are used. These expressions can be used for security purposes.

**Keywords-component; Fisher's linear discriminant function, Wavelet Gabor filter.**

### I. INTRODUCTION

Man communicates to another person using expressions. In this expression, words are mixed along with facial muscle movements. Computers are "emotionally challenged". The universal expressions are classified based on Love-fear. Some of the basic expressions are angry, happy, fear, disgust, sad, surprise and neutral. There can be many types of unlimited expressions which can be observed from the face of actors and actress. They are embarrassments, interest, pain, shame, shy, anticipation, smile, laugh, sorrow, hunger, curiosity. Different techniques can be adapted for expressing anger. This can be like Enraged, annoyed, anxious, irritated, resentful, miffed, upset, mad, furious, and raging. Similarly, Happy can be through joy, greedy, ecstatic, fulfilled, contented, glad, complete, satisfied, and pleased.

In addition, Disgust be presented by contempt, exhausted, peeved, upset, and bored. The angry can be shown through brows by lowering and drawing together, with Vertical lines appearing between the brows, lower lid highly

tensed, eyes hard stare or bulging, lips can be pressed firmly together with corners down. During happiness, the corners of the lips appear to be drawn back and up. The mouth is parted with teeth exposed. A wrinkle runs from the outer nose to the outer lip. Meanwhile, the cheeks are raised, and the lower lid shows wrinkles.

### II. RELATED WORK

Standard methods like static and dynamic techniques have been used earlier by researchers in identifying expressions. Bayesian technique has been used as an important static method. Ravi et al, 2011, gave a comparative study and analysis of 'Facial Expression Recognition Technology' along with its progressive growth and developments. Oliveira et al., 2011, proposed a novel method called two-dimensional discriminant locality preserving projections (2D-DLPP) is proposed that can best discriminate different pattern classes. Cheng et al., 2011, proposed a Gaussian Process model for the facial expression recognition in the Japanese female facial expression dataset and found successful classification of facial expression.

Klaus and Ursula, 2011, report the development of a rapid test of expression recognition ability, the Emotion Recognition Index (ERI), consisting of two subtests: one for facial and one for vocal expression recognition. Ruffman, 2011, presents that recognition of expression in still photos provides important information about young-old differences, and has sufficient ecological validity to explain age differences in a number of social insights. Bänziger et al., 2012, discusses an overview of some of the major emotion expression (EE) corpora currently available for empirical research and introduces a new, dynamic, multimodal corpus of expression expressions, the Geneva Multimodal Emotion Portrayals Core Set (GEMEP-CS). Schlegel et al., 2012, studied on expression recognition ability (ERA) that can inform the measurement of the expression perception component in emotional intelligence.

### III. PROBLEM DEFINITION

Many techniques have been developed over a period of facial expression recognition and applied for various situations. In

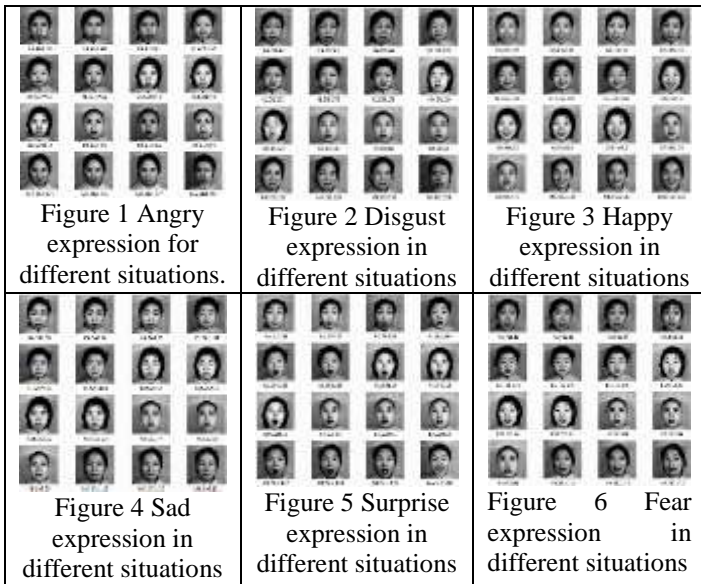
this paper, an effort is made to know the feasibility of identifying expressions from South Indians.

#### IV. THE SYSTEM SETUP

The implementation of the expression identification system includes detection of the image, training the images for recognition and testing the image for identification

##### 1. Image Detection

A face has to be detected in a captured image. Once detected, the image region containing the face is extracted and geometrically normalized. Images have been acquired using a standard digital camera. The expression of a person under different conditions are presented in Figures 1-6 shows some of the training images.



The statistical values of the frames of each facial expression are presented in Figures 7-12. The summed difference between adjacent frames is plotted for the expression “Angry” in Figure7.

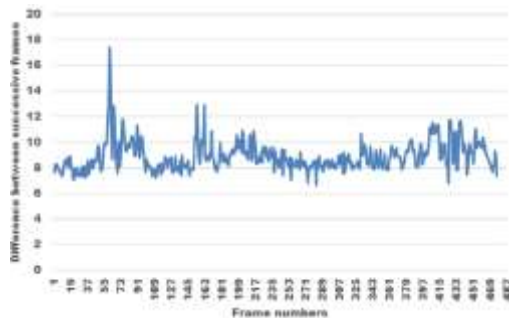


Figure 7 Difference values for the expression ‘Angry’

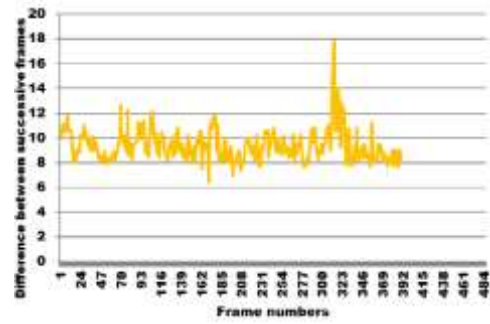


Figure 8 Difference values for the expression ‘Disgust’

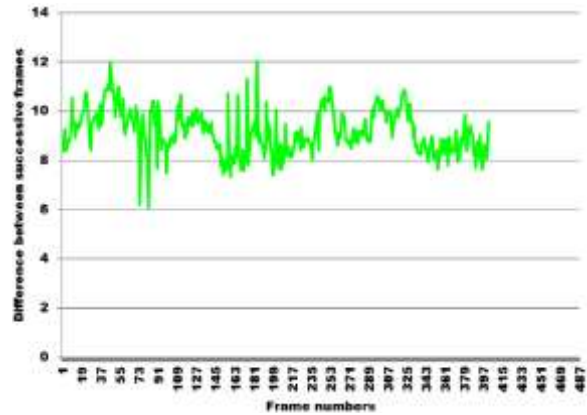


Figure 9 Difference values for the expression ‘Fear’

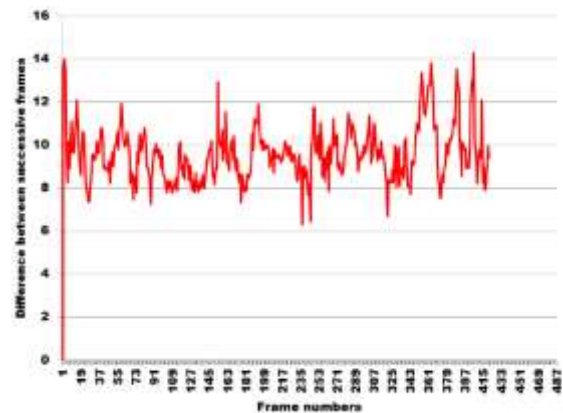


Figure 10 Difference values for the expression ‘Happy’

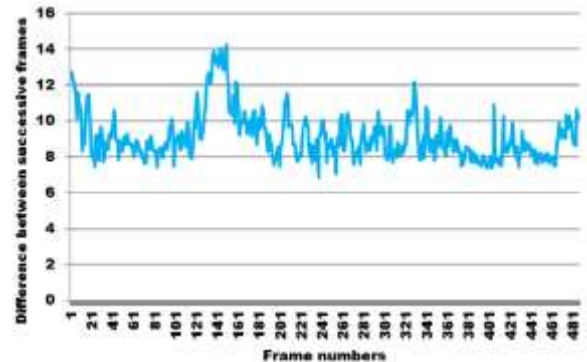


Figure 11 Difference values for the expression ‘Sad’

2. Feature Extraction by Rotational Wavelet Gabor Filter

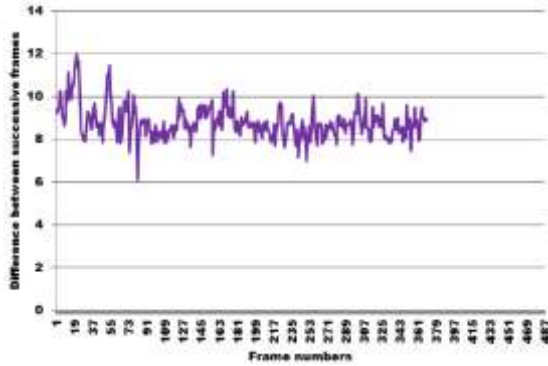


Figure 12 Difference values for the expression ‘Surprise’

The Figures 6-12 show that there are some variations of information in the successive frames. In reality, the variations can be due to change in the lighting conditions, or other factors. However, we have assumed that the lighting conditions are constant. Hence, the difference in variations of the graph indicates some movements in the skin of the face and movement in the lips. The person does not move her head rather than the only face.

The Figure 13 indicates there is overlapping of the difference values calculated for the successive frames for all the six expressions. The plot shows there is a variation in the contents of the frames.

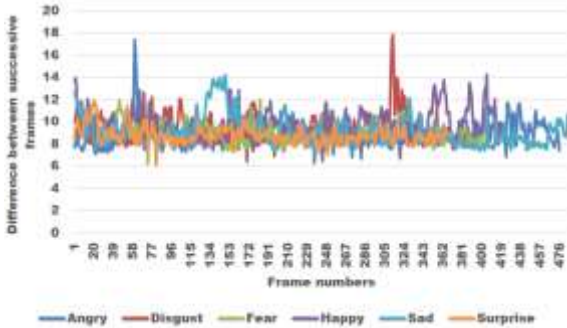


Figure 13 Comparisons of the difference values of the successive frames for six facial expression expression (FEE)

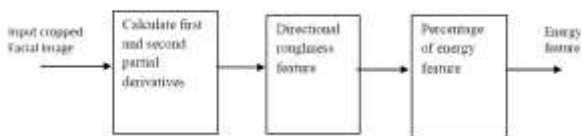


Figure 14 Design of feature extraction

Facial texture segmentation plays an important role in recognizing and identifying a material, type of characteristic for particular image. Wavelets are employed for the computation of single and multi-scale roughness features because of their ability to extract information at different resolutions. Features are extracted in multiple directions using directional wavelet obtained from partial derivative of Gaussian distribution function. The first and second derivative wavelets are used to obtain the features of the textured image at different orientations like 0°, 45°, 90° and 135° and scales such as 1, 2 and 4.

Facial segmentation procedure partition an image into constituent object that is used to find the regions of interests using K-means algorithm. The schematic flow of the extracting energy feature from the textured image is given in figure 14.

2.1. PREPROCESSING

Preprocessing is done for the removal of noise from image using Gaussian smoothing function. In designing Gaussian filters the mask weights are computed directly from the Gaussian distribution, given by equation (1)

$$\phi(x, y, s) = \exp\left\{-\frac{x^2 + y^2}{2s^2}\right\} \tag{1}$$

Where x, y are directions, and s is the scale

An overlapping moving window size of NxN is used for preprocessing. The coefficient value at the center of the mask is made equal to one by a suitable multiplication factor. When performing the convolution, the output pixel values must be normalized by the sum of the mask weights to ensure that regions of uniform intensity are not affected.

2.2 Directional roughness feature

A wavelet from the exponential wavelet family is used for the computation of roughness features. The 2-D Gaussian smoothing function from equation (1) is partially differentiated with respect to x and y to calculate the first order partial derivatives of the smoothing function along x-axis and y-axis.

Along x-direction (0°)

$$W_0(x, y, s) = \frac{\partial\phi(x, y, s)}{\partial x} = \frac{-x}{s} \exp\left\{-\frac{x^2 + y^2}{2s^2}\right\} \tag{2}$$

Along y-direction (90°)

$$W_{90}(x, y, s) = \frac{\partial\phi(x, y, s)}{\partial y} = \frac{-y}{s} \exp\left\{-\frac{x^2 + y^2}{2s^2}\right\} \tag{3}$$

Gradient component or the filtered version of the original image in direction 0° and 90° is calculated by convolving the

original image  $f(x,y)$  with the partial derivative filters along  $x$  and  $y$  directions.

$$W_0(x,y,s) * f(x,y) = \frac{\partial \phi(x,y,s)}{\partial x} * f(x,y) \quad (4)$$

$$W_{90}(x,y,s) * f(x,y) = \frac{\partial \phi(x,y,s)}{\partial y} * f(x,y) \quad (5)$$

The filtered version of the original image along other directions other than  $0^\circ$  and  $90^\circ$  is calculated by using the linear combination of equations 4 and 5 and is given in equation (6)

$$W_\theta(x,y,s) * f(x,y) = [W_0(x,y,s) * f(x,y)] \cos \theta + [W_{90}(x,y,s) * f(x,y)] \sin \theta \quad (6)$$

Where  $\theta$  - is the directional angle

Similarly, the second order partial derivatives of the smoothing function is calculated along the directions  $(0^\circ, 90^\circ)$ ,  $(0^\circ, 0^\circ)$  and  $(90^\circ, 90^\circ)$ . The second order partial along the direction  $(0^\circ, 90^\circ)$  is obtained by partially differentiating  $W_0(x, y, s)$  with respect to  $x$  as given in equation (7)

$$W_{0,90}(x,y,s) = \frac{\partial^2 \phi(x,y,s)}{\partial x \partial y} = \frac{xy}{s^4} \exp\left\{-\frac{x^2 + y^2}{2s^2}\right\} \quad (7)$$

The second order partial along the direction  $(0^\circ, 0^\circ)$  is obtained by partially differentiating  $W_0(x, y, s)$  with respect to  $x$  as given in equation (8)

$$W_{0,0}(x,y,s) = \frac{\partial^2 \phi(x,y,s)}{\partial^2 x} = \left(\frac{x^2}{s^4} - \frac{1}{s^2}\right) \exp\left\{-\frac{x^2 + y^2}{2s^2}\right\} \quad (8)$$

The partial along the direction  $(90^\circ, 90^\circ)$  is obtained by partially differentiating  $W_{90}(x, y, s)$  with respect to  $y$  as given in equation (9)

$$W_{90,90}(x,y,s) = \frac{\partial^2 \phi(x,y,s)}{\partial^2 y} = \left(\frac{y^2}{s^4} - \frac{1}{s^2}\right) \exp\left\{-\frac{x^2 + y^2}{2s^2}\right\} \quad (9)$$

The filtered version of the original image along other directions is obtained by the linear combination of the equations 7, 8 and 9 as given in equation (10)

$$W_{\theta, \theta+90}(x,y,s) * f(x,y) = [W_{0,90}(x,y,s) * f(x,y)] * \cos 2\theta + 0.5 * \left\{ [W_{0,0}(x,y,s) * f(x,y)] - [W_{90,90}(x,y,s) * f(x,y)] \right\} \sin 2\theta \quad (10)$$

The gradient component along any directions is found by using the equations 6 and 10. The two wavelet transforms of a function  $f(x,y)$  at scale  $s$  and direction  $\theta$  are calculated as given in equation (11)

$$W_1 T_f^\theta(x,y,s) = W_0(x,y,s) * f(x,y)$$

$$W_2 T_f^\theta(x,y,s) = W_{\theta, \theta+90}(x,y,s) * f(x,y) \quad (11)$$

where

$W_1 T_f^\theta(x, y, s)$  – is the first derivative wavelet

$W_2 T_f^\theta(x, y, s)$  – is the second derivative wavelet.

Figure 15-17 show the directional values along  $y$ -axis for different angle of rotations of Gabor filter. The  $x$ -axis shows the different locations of the image. Figure 18 shows the final output of the Gabor wavelet output.

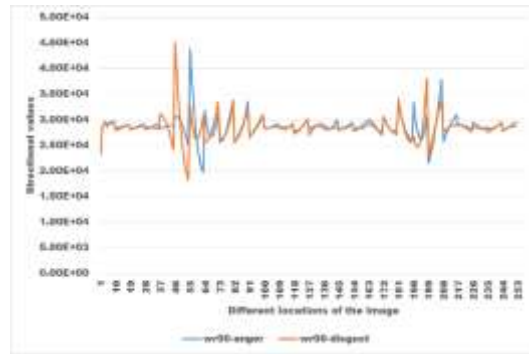


Figure 15 Directional values along wr00

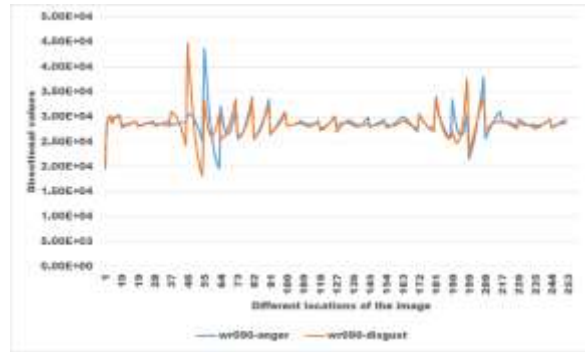


Figure 16 Directional values along wr090

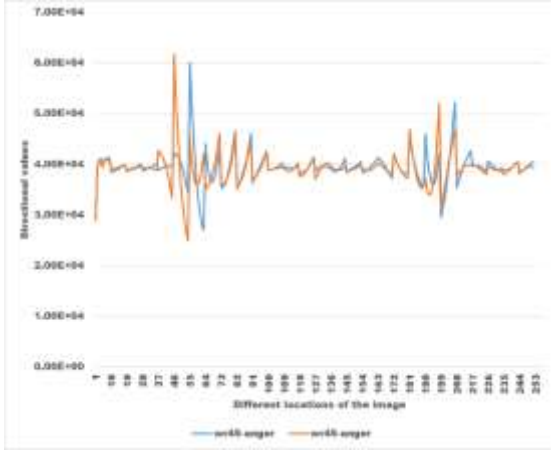


Figure 17 Directional values along wr45

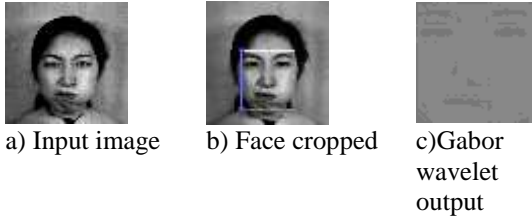


Figure 18 Final output of wavelet Gabor texture extraction

### 2.3 The directional roughness features ( $R_s^\theta$ )

The directional roughness features is obtained by finding the arithmetic average in a  $9 \times 9$  window for the two wavelet transforms given in the equations 11 and 12 with different orientations and scales. The wavelet with the maximum is selected as given in equation (13)

$$R_s^\theta \approx \langle \max |W_i T_f^\theta(u, v, s)| \rangle_{N \times N} \quad (13)$$

$\langle \rangle_{N \times N}$  – arithmetic average in an  $N \times N$  window  
 $i = 1, 2$  (1 and 2 derivative wavelet)

### 2.4 Percentage of energy feature

The effect of roughness depends on the relative texture energy between different directions. The roughness features are weighted with the percentage of textural energy existing in the corresponding direction. The energy computed in direction  $\theta$  using an  $s$ -scale wavelet is given by equation (14).

$$E_{s,i}^\theta = \langle |W_i T_f^\theta(x, y, s)| \rangle_{N \times N} \quad (14)$$

#### Total Energy

The total energy at scale  $s$  is obtained from equation (15)

$$E_s^{total} = \sum_{\theta} \langle |W_i T_f^\theta(x, y, s)| \rangle_{N \times N} \quad (15)$$

#### 4.2.5.1 Percentage of Energy

The percentage of energy feature computed in direction  $\theta$  and scale  $s$  is given by equation

$$\text{Per}_{s,i}^\theta = \frac{E_s^\theta}{E_s^{total}} \quad (16)$$

where

$E_s^\theta$  is the energy computed in direction  $\theta$

$E_s^{total}$  is the total energy

The percentage of energy  $\text{Per}_{s,i}^\theta$  is insensitive to the absolute image illumination because energy is computed using exponential wavelets where the dc component is removed. It is also insensitive to contrast changes, because  $E_s^\theta$  and  $E_s^{total}$  is multiplied by a constant multiplicative term.

The output of wavelet Gabor filter is used as input for Fisher's linear discriminant function for obtaining transformed higher dimensional feature vector into two dimensional vector by computation of discriminant vectors  $\phi_1$  and  $\phi_2$

The Fisher's criterion is given by

$$J(\phi) = \frac{\phi^T S_b \phi}{\phi^T S_w \phi} \quad (17)$$

$$S_b = \sum_{i=1}^m P(\omega_i) (m_i - m_o)(m_i - m_o)^T \quad (18)$$

$$S_w = \sum_{i=1}^m P(\omega_i) E[(x_i - m_i)(x_i - m_i)^T / \omega_i] \quad (19)$$

Where

$S_b$  is the between class matrix, and

$S_w$  is the within class matrix which is non-singular.

$P(\omega_i)$  is a priori the probability of the  $i^{\text{th}}$  pattern,  $P(\omega_i) = 1/m$ ,

$m_i$  is the mean vector of the  $i^{\text{th}}$  class patterns,  $i=1, 2, \dots, m$ ;

$m_o$  is the global mean vector of all the patterns in all the classes.

$X = \{X_i, i=1, 2, \dots, L\}$  is the  $n$ -dimensional patterns of each class.

The discriminant vector that maximizes  $J$  in equation (17) is denoted by  $\phi_1$ . The vector  $\phi_1$  is found as a solution of the Eigenvalue problem given by equation (20).

$$S_b \phi_1 = \lambda_{m1} S_w \phi_1 \quad (20)$$

Where  $\lambda_{m1}$  is the greatest non-zero eigenvalue of  $S_b S_w^{-1}$ . The eigenvector corresponding to  $\lambda_{m1}$  is  $\phi_1$ . Another discriminant vector  $\phi_2$  is obtained by using the same criterion of equation (17). The vector  $\phi_2$  should also satisfy the equation given by equation (21).

$$\phi_2^T \phi_1 = 0.0 \quad (21)$$

The equation (21) indicates that the solution obtained is geometrically independent. The discriminant vector  $\phi_2$  is found as a solution of the Eigen value problem, which is given by equation (22).

$$Q_p S_b \phi_2 = \lambda_{m2} S_w \phi_2 \quad (7 \quad 22)$$

Where

$\lambda_{m2}$  is the greatest non-zero eigenvalue of  $Q_p S_b S_w^{-1}$  and  $Q_p$  is the projection matrix given by equation (23).

$$Q = I - \frac{\phi_1 \phi_1^T S_w^{-1}}{\phi_1^T S_w^{-1} \phi_1} \quad (23)$$

Where,  $I$  is an identity matrix. Figure 19 shows the effect of eigenvalue in differentiating the different expressions. Eigen value for three different frames of three different expressions are plotted in Figure 19 that indicate distinguished difference among different facial images, This is an indication that, eigenvalue process can be applied for facial image identification.

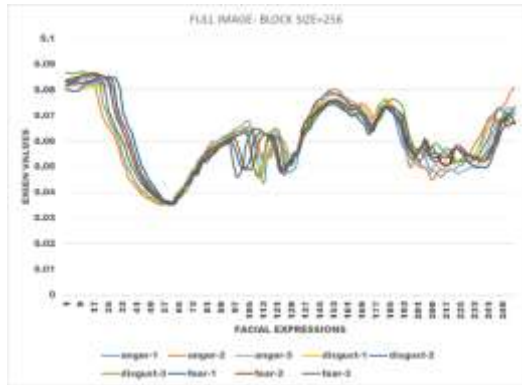


Figure 19 Eigen value plot for different frames

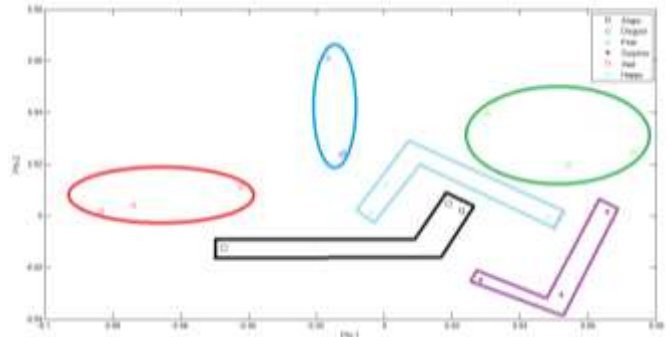


Figure 20 Plot of discriminant vectors for all six expressions

In equation (22),  $S_w$  should be non-singular. It is necessary that  $S_w$  should be non-singular, even for a more general discriminating analysis and generating multi orthonormal vectors, If  $S_w$  is singular,  $S_w$  should be made on-singular, by using singular value decomposition (SVD) method and perturbing the matrix. By using equations (20 and 22), the values of  $\phi_1$  and  $\phi_2$  discriminant vectors are obtained and presented in Figure 20. In this figure, the expressions happy and sad are scattered and not cluttered. The other expressions are cluttered.

The 2-dimensioal vectors set are denoted by  $Y_i$ . The vector  $Y_i$  is given by equation (24).

$$Y_i = (u_i, v_i) = \{ X_i^T \phi_1, X_i^T \phi_2 \} \quad (24)$$

The vector set  $Y_i$ , is obtained by projecting the original vector 'X' of the patterns onto the space spanned by  $\phi_1$  and  $\phi_2$  by using equation 24.

## V. CONCLUSION

In this paper, sample images with expressions are used for training and testing the proposed system of expression identification. Wavelet Gabor filter, Fisher's linear discriminant function are used to implement the system. The performance of the system is purely based on the quality of the images. The future work includes in analyzing the proposed system and its suitability for people with different origins.

## REFERENCES

- [1] Bänziger, T., Mortillaro, M., & Scherer, K. R. (2012). Introducing the Geneva Multimodal expression corpus for experimental research on emotion perception. *Emotion*, 12, 1161–1179. doi:10.1037/a0025827.
- [2] Cheng, F. , Yu, J. , & Xiong, H. (2010). Facial expression recognition in jaffe dataset based on Gaussian process classification. *IEEE Transactions on Neural Networks*, 572 21(10), 1685–1690.
- [3] Klaus R. Scherer and Ursula Scherer, 2011, Assessing the Ability to Recognize Facial and Vocal Expressions of Emotion: Construction and Validation of the Emotion Recognition Index, *J Nonverbal*

- Behav., Vol.35, pp.305–326., DOI 10.1007/s10919-011-0115-4.
- [4] Oliveira, L. E. S. , Koerich, A. L. , Mansano, M. , & Britto, A. S. Jr. , (2011). 2d principal component analysis for face and facial expression recognition. *Computing in Science and Engineering*, 13(3), 9–13.
- [5] Ravi S., and Mahima S., 2011, Study of the Changing Trends in Facial Expression Recognition, *International Journal of Computer Applications* (0975-8887), Vol.21. No.5, pp.10-16.
- [6] Ruffman, T. (2011). Ecological validity and age-related change in emotion recognition. *Journal of Nonverbal Behavior*, 35, 297–304. doi:10.1007/s10919-011-0116-3
- [7] Schlegel, K., Grandjean, D., & Scherer, K. R. (2012). Emotion recognition: Unidimensional ability or a set of modality- and emotion-specific skills? *Personality and Individual Differences*, 53, 16–21. doi:10.1016/j.paid .2012.01.026.